Electronic Supplementary Material (ESI) for Nanoscale.
This journal is © The Royal Society of Chemistry 2018

Supporting Information

Engineering Stereo-film of $FeNi_3$ Nanosheet-covered FeOOH arrays for Efficient Oxygen Evolution

Huiyuan Meng, Zhiyu Ren, Shichao Du, Jun Wu, Xu Yang, Yuzhu Xue and Honggang Fu**

Table of contents

1. Supplementary Figures 2
Figure S1 2
Figure S2 2
Figure S3 2
Figure S4 3
Figure S5 3
Figure S6 4
Figure S7 4
Figure S8 5
Figure S9 5
Figure S10 5
Figure S11 6
Figure S12 6
Figure S13 7
Figure S14 7
Figure S15 8
Figure S16 8
Figure S17 8
2. Supplementary Tables 9
Table S1 9
Table S2 10
Table S3 14
Table S4 15

1. Supplementary Figures

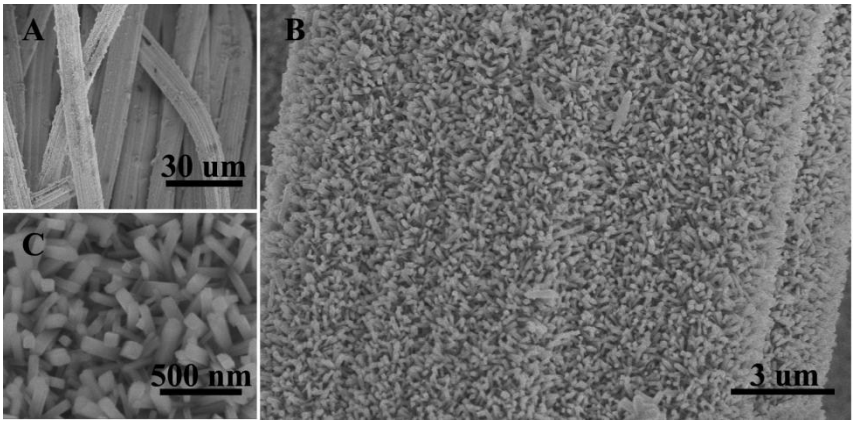

Figure S1. SEM images of FeOOH-CC.

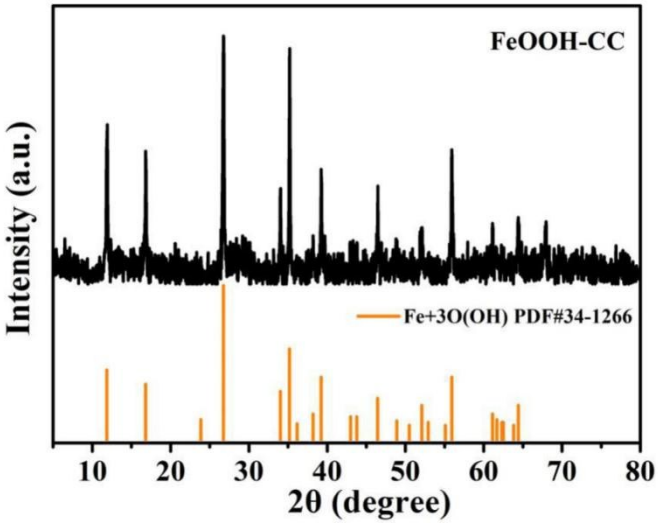

Figure S2. XRD pattern of FeOOH-CC.

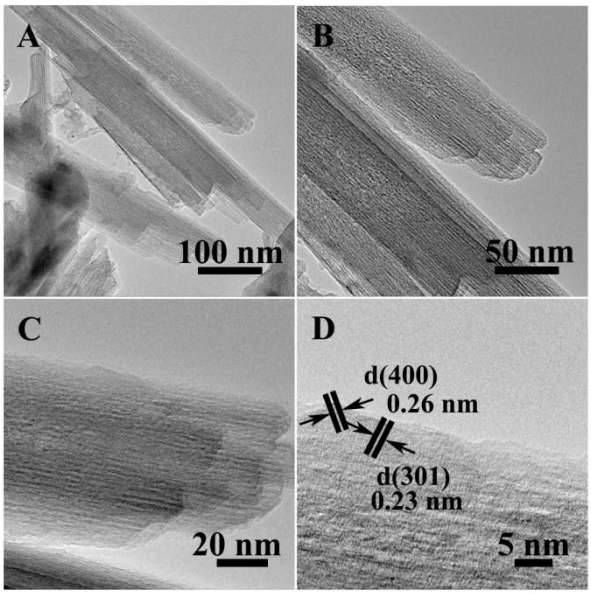

Figure S3. TEM images of FeOOH.

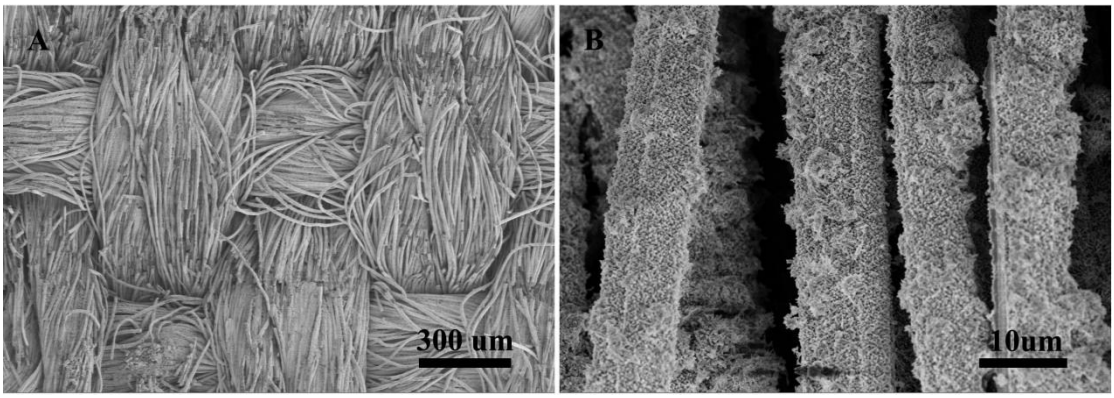

Figure S4. SEM images of F@$FeNi_3$-CC-3 obtained after the reductive electrodeposition at -1.2 V (vs. Ag/AgCl) for 600 s.

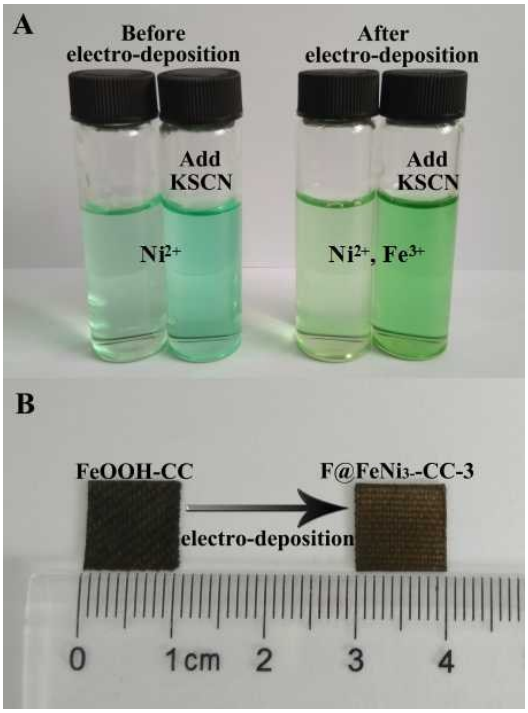

Figure S5. (A) The optical photographs of electrolyte before and after reductive electrodeposition at -1.2 V (vs. Ag/AgCl) for 600 s. (B) The optical photographs of FeOOH-CC and F@$FeNi_3$-CC-3.

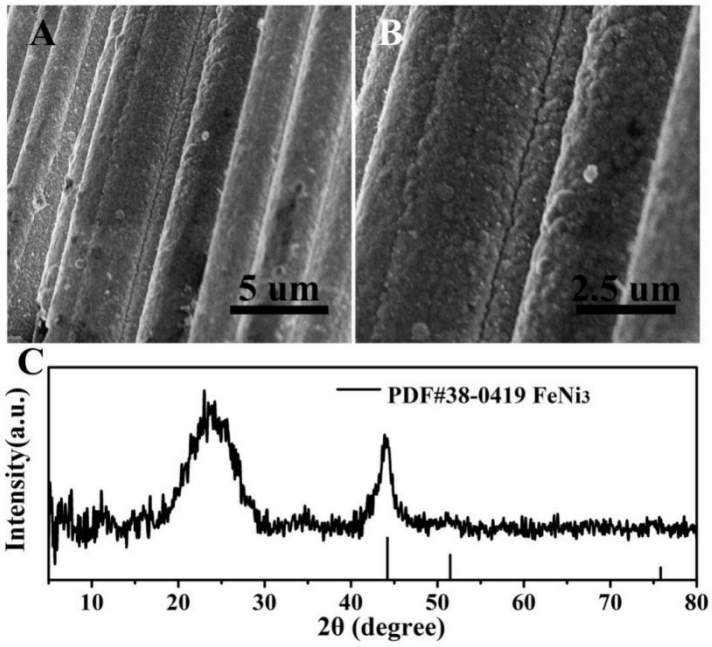

Figure S6. (A and B) SEM images of $FeNi_3$-CC obtained after the reductive electrodeposition at -1.2 V (vs. Ag/AgCl) for 600 s (the mol ratio of Fe^{3+} and Ni^{2+} in the electrolyte is 3:1). (C) XRD pattern of $FeNi_3$-CC.

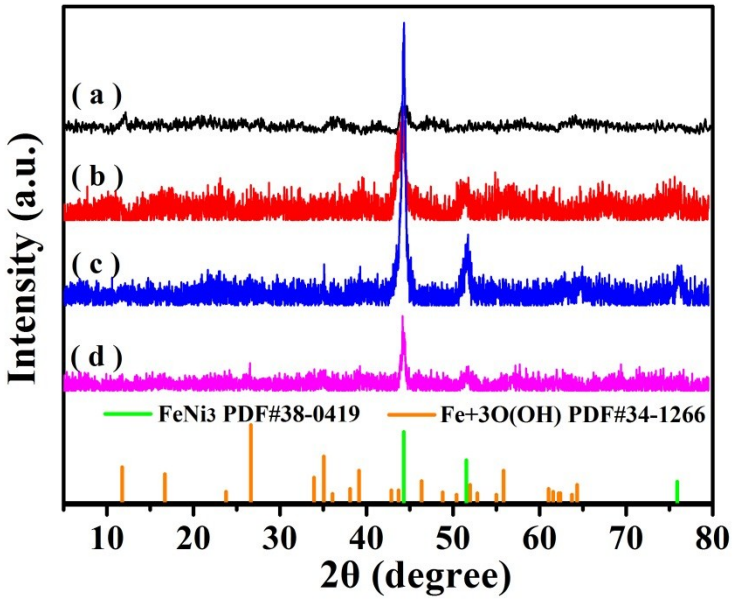

Figure S7. XRD patterns of F@FeNi-CC obtained after electrodeposition at various potentials; (from a to d) the electrodeposition potential is -1.0, -1.1, -1.3, and -1.4 V (*vs.* Ag/AgCl), respectively.

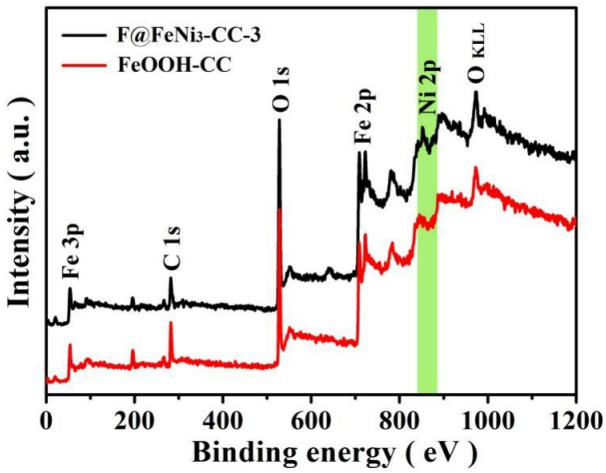

Figure S8. XPS spectra of FeOOH-CC and F@$FeNi_3$-CC-3.

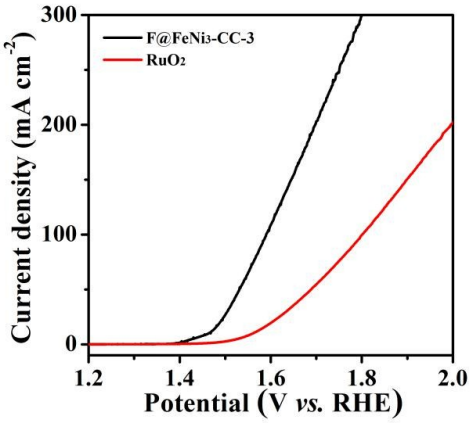

Figure S9. OER polarization curves for $FeNi_3$-CC-3 and RuO_2 in 1.0 M KOH (scan rate: 1 mV s^{-1}), respectively.

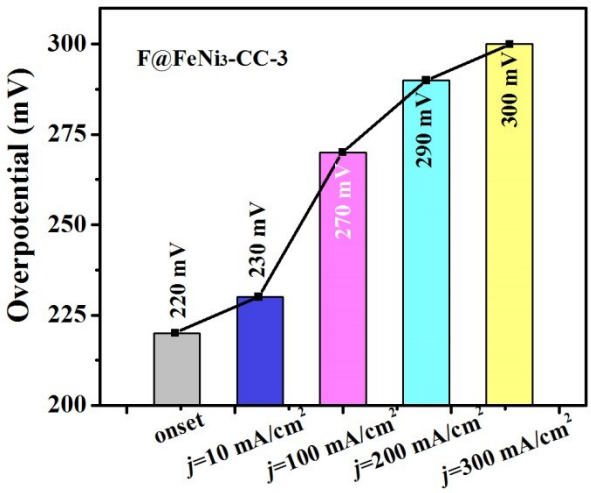

Figure S10. OER onset overpotential and overpotential of F@$FeNi_3$-CC-3 required for various current density, respectively.

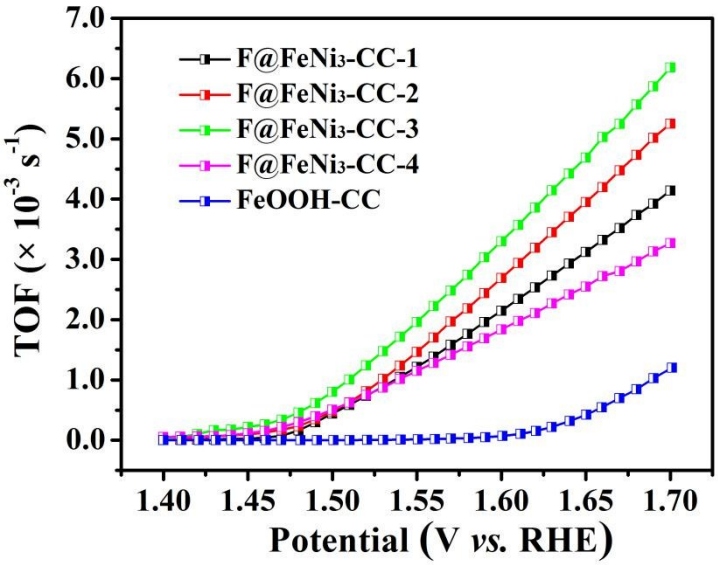

Figure S11. TOFs with respect to all Fe and Ni ions of F@$FeNi_3$-CC-x and FeOOH-CC at different potentials.

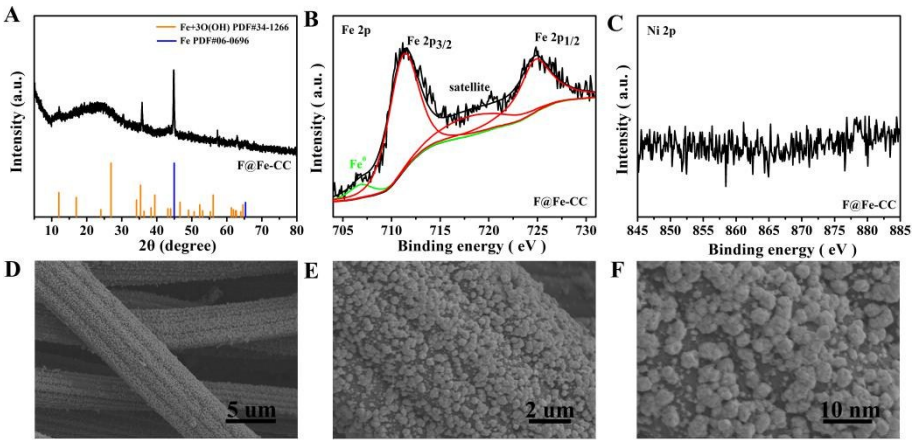

Figure S12. (A) XRD patterns of F@Fei-CC; (B, C) the high-resolution Fe *2p* and Ni *2p* XPS spectra of of F@Fe-CC; (D-F) the SEM images of F@Fe-CC.

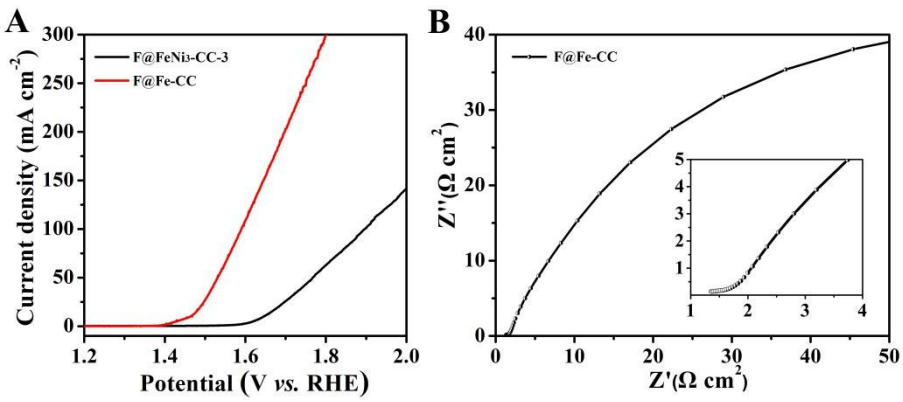

Figure S13. OER polarization curves for F@Fe-CC in 1.0 M KOH (scan rate: 1 mV s^{-1}); Nyquist plots of F@Fe-CC in 1.0 M KOH, under OER overpotential = 220 mV.

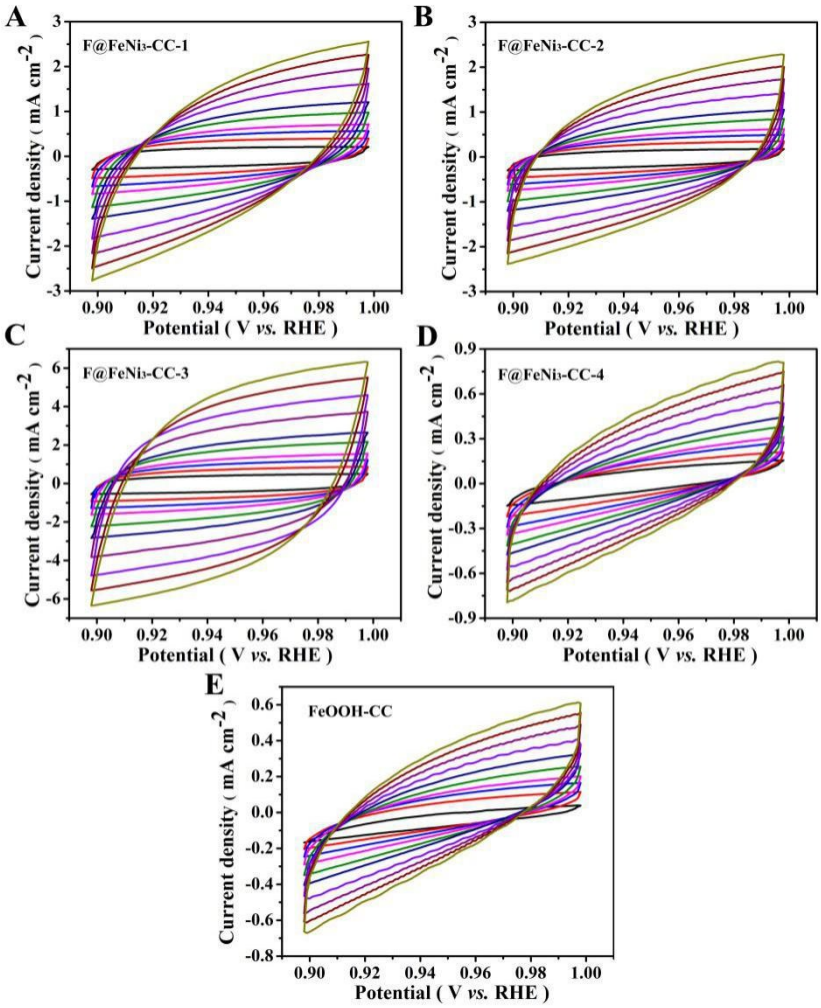

Figure S14.. (A-F) CVs for F@$FeNi_3$-CC-1, F@$FeNi_3$-CC-2, F@$FeNi_3$-CC-3, F@$FeNi_3$-CC-4, and FeOOH-CC at different scan rate from 5 to 200 mV s^{-1}, respectively.

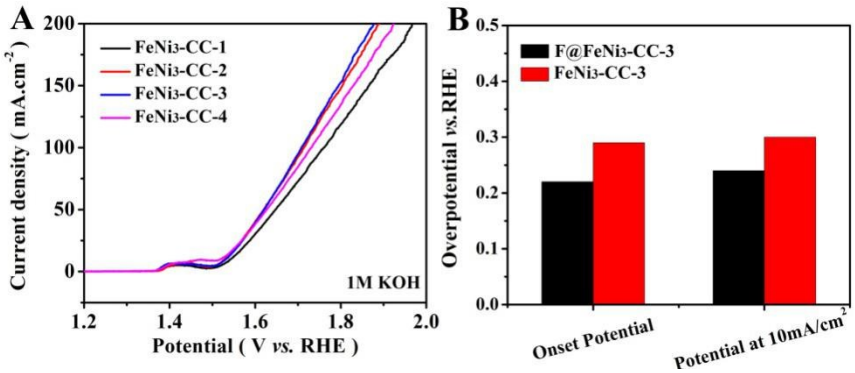

Figure S15. (A) OER polarization curves for $FeNi_3$-CC-1, $FeNi_3$-CC-2, $FeNi_3$-CC-3, and $FeNi_3$-CC-4 in 1.0 M KOH (scan rate: 1 mV s^{-1}), respectively; (B) the OER onset overpotential and overpotential required for j = 10 mA cm^{-2} of $FeNi_3$-CC-3 and F@$FeNi_3$-CC, respectively.

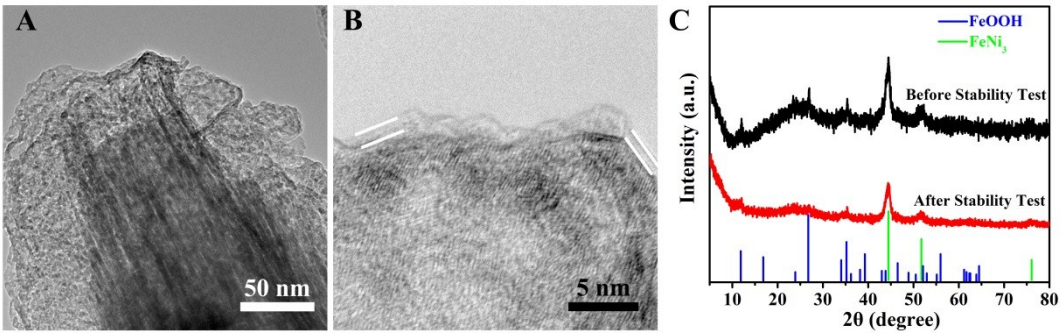

Figure S16. (A and B) TEM images of F@$FeNi_3$-CC-3 after 100 h OER measurements at a current density of 10 mA cm^{-2} in 1.0 M KOH; (C) XRD patterns of F@$FeNi_3$-CC-3 before and after stability test.

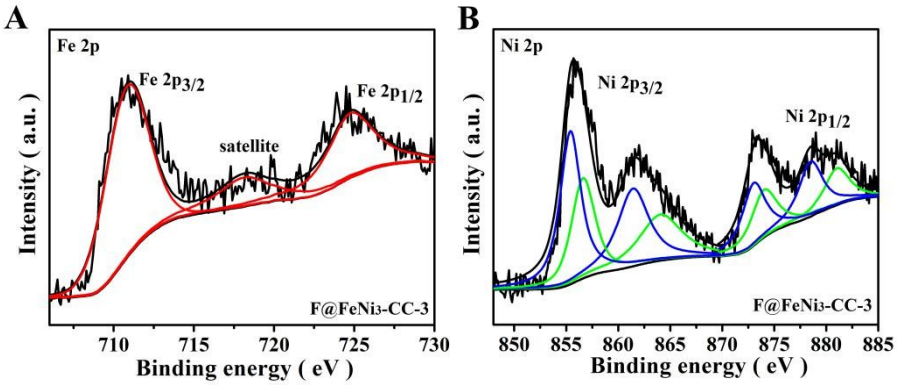

Figure S17. (A and B) The high-resolution Fe 2p and Ni 2p XPS spectra of F@$FeNi_3$-CC-3 after 100 h OER measurements at a current density of 10 mA cm^{-2} in 1.0 M KOH.

2. Supplementary Tables

Table S1. The ICP-AES results of various F@$FeNi_3$-CC-x and FeOOH-CC.

Samples	Fe (mmol/cm^2)	Ni (mmol/cm^2)
FeOOH-CC	**0.048**	**---**
F@$FeNi_3$-CC-1	**0.047**	**0.0098**
F@$FeNi_3$-CC-2		**0.017**
F@$FeNi_3$-CC-3		**0.035**
F@$FeNi_3$-CC-4		**0.039**

Table S2. Comparison of OER performance of F@$FeNi_3$-CC-3 with recently reported Fe- and Ni-based electrocatalysts in alkaline electrolyte.

Catalysts	Substrate	η at 10 mA·cm^{-2} (mV)	Tafel slope (mV/dec)	Electrolyte	Reference
F@$FeNi_3$-CC-3	***CC***	***230***	***47***	***1.0 M KOH***	***This work***
$Ni(OH)_2/\gamma$-NiOOH	Au disc	280	---	1 M KOH	J. Phys. Chem. C 2015, 119, 7243
Ni_3Se_2 films	Ni foam	270	142	0.3 M KOH	Energy Environ. Sci. 2016, 9, 1771
Ni_3C/C hybrid composite	GCE	280 (2)	46	1 M KOH	Adv. Mater. 2016, 28, 3326
Ni-NiO/N-rGO	GCE	240	43	0.1 M KOH	Adv. Funct. Mater. 2015, 25, 5799
Ni-Bi@Ni_3B	GCE	302	52	1 M KOH	Angew. Chem. Int. Ed. 2017, 56, 6572
α-$Ni(OH)_2$ nanocrystals	GCE	331	42	0.1 M KOH	J. Am. Chem. Soc. 2014, 136, 7077
$Ni(OH)_2/\gamma$-NiOOH	Au disc	280	---	1 M KOH	J. Phys. Chem. C 2015, 119, 7243
carbon coated porous nickel phosphides nanoplates	GCE	200	64	1 M KOH	Energy Environ. Sci. 2016, 9, 1246
Fe/N/C and bimetallic metal-organic framework composites	GCE	410	---	0.1 M KOH	ACS Appl. Mater. Interfaces 2017, 9, 5213
Fe-Pi	Ni foam	215	28	1 M KOH	J. Mater. Chem. A 2017, 5, 18627
Fe-N-codoped graphene	GCE	440	96	0.1 M KOH	J. Mater. Chem. A 2017, 5, 1930
amorphous $FePO_4$ nanosheet	Ni foam	310	42.72	1 M KOH	Adv. Mater. 2017, 29, 1704574
Fe-based binary diselenide-derived oxide	GCE	226	41	0.1 KOH	ACS Appl. Mater. Interfaces 2017, 9, 40351
$FeSe_2$	Ni foam	245	---	1 M KOH	Angew. Chem. Int. Ed. 2017, 56, 10506
atomic dispersion of Fe-N_x species on N and S co-decorated hierarchical carbon layers	GCE	370	82	0.1 M KOH	Angew. Chem. Int. Ed. 2017, 56, 610
Fe_2P/Fe_4N@N-doped carbons	GCE	410	177	1 M KOH	ACS Appl. Mater. Interfaces 2017, 9, 32840
FeOOH/CeO_2 heterolayered nanotube	Ni foam	210 (2)	92.3	1 M NaOH	Adv. Mater. 2016, 28, 4698
$Fe_{0.4}Co_{0.6}$ composite films	CFP	283	34	1 M KOH	Nano Energy 2017, 38, 576
FeCoP urban nano-sheet arrays	Ni foam	260 (20)	63	1 M KOH	Nano Energy 2017, 41, 583
Au@$CoFeO_x$	GCE	328	---	1 M KOH	Nano Lett. 2017, 17, 6040
Fe-doped CoP nanosheet array	CC	280 (20)	---	1 M KOH	Chem. Commun. 2017, 53, 5710
mesoporous nickel cobalt oxide	GCE	336	36	1 M KOH	ACS Appl. Mater. Interfaces 2017, 9, 21225
NiCo bimetal-organic framework nanosheets	Cu foam	189	42	1 M KOH	Nat. Energy 2016, 1, 16184
Fe-doped CoP nanoarray	Ti foil	230	67	1 M KOH	Adv. Mater. 2017, 29, 1602441
$CoFe_2O_4$/CoO	GCE	320	71	1 M KOH	Scientific Reports.2017, 7, 13161

hexagonal sphericon hematite-modifed Ce-Ni	GCE	340	45	0.1 M KOH	Adv. Mater. 2017, 29, 1703792
$CoFe_2O_4$/C porous hybrid nanorod arrays	Ni foam	240	45	1 M KOH	Adv. Mater. 2017, 29, 1604437
Co-Ni-based nanotubes/nanosheets	Cu foil	280	77	1 M KOH	Adv. Energy Mater. 2016, 6, 1501661
Fe-doped porous cobalt phosphide polyhedrons	GCE	289	66	1 M KOH	Small 2017, 13, 1701167
Ni-Co mixed metal phosphide nanoboxes	GCE	330	96	1 M KOH	Angew. Chem. Int. Ed. 2017, 56, 3897
FeOOH/Co/FeOOH hybrid nanotube arrays	Ni foam	250 (20)	32	1 M NaOH	Angew. Chem. Int. Ed. 2016, 55, 3694
$Ni_{0.8}Fe_{0.2}O_xH_y$ film	CC	-	37	1 M KOH	Chem. Mater. 2017, 29, 120
$Ni_xFe_{1-x}OOH$/NiFe/$Ni_xFe_{1-x}OOH$ sandwich-structured nanotube arrays	CFC	220	57	1 M KOH	ACS Appl. Mater. Interfaces 2017, 9, 34954
Ni-Fe LDHs nanosheets intercalated with molybdate anions	Ni foam	280	40	1 M KOH	J. Mater. Chem. A 2015, 3, 16348
NiFeOH@NF	Ni foam	210	31	1 M KOH	J. Mater. Chem. A 2017, 5, 11009
NiFe LDH-NS@DG10 hybrid	GCE	210	52	1 M KOH	Adv. Mater. 2017, 29, 1700017
Ultrathin NiFe-LDH nanoplatelets	Ni foam	224	52.8	1 M KOH	Chem. Sci. 2015, 6, 6624
stacked NiFe hydroxide nanosheets and graphene	GCE	230	40	1 M KOH	ACS Nano 2015, 9, 1997
FeOOH/NiFe LDHs	Ni foam	208	---	1 M KOH	ACS Appl. Mater. Interfaces 2017, 9, 464
mesoporous NiFe-oxide nanocube	CFP	271	48	1 M KOH	ACS Appl. Mater. Interfaces 2017, 9, 41906
porous Ni-Fe mixed oxides	GCE	328	42	0.1 M KOH	Adv. Sci. 2015, 2, 1500199
Ni-Fe-OH@Ni_3S_2 nanoarrays	Ni foam	165	93	1 M KOH	Adv. Mater. 2017, 29, 1700404
$NiFeO_x$ flake	Ni foam	210	---	1.5 M $KHCO_3$	Angew. Chem. Int. Ed. 2017, 56, 5061
NiFe@NC	GCE	350	56	0.1 M KOH	Nano Energy 2016, 30, 426
$Ni_{1.5}Fe_{0.5}P$	CF	359	55	1 M KOH	Nano Energy 2017, 34, 472
$NiFeS_2$ arrays	Ni Foam	215	28	1 M KOH	Nano Energy 2017, 41, 148
Ni-Fe@rGO	GCE	350	38	0.1 M KOH	Langmuir 2017, 33, 2
Fe-doped Ni_2P nanosheet arrays	Ni foam	270 (20)	96	1 M KOH	ACS Appl. Mater. Interfaces 2017, 9, 26001
Fe-Ni-P/rGO	GCE	240	63	1 M KOH	ACS Appl. Mater. Interfaces 2017, 9, 23852
amorphous mesoporous NiFe nanosheets	Ni foam	215	32	1 M KOH	Nature Communications. 2015, 6, 7616
FeNi@NC	GCE	280	70	1 M NaOH	Energy Environ. Sci. 2016, 9, 123
$Ni_{1-x}Fe_xPS_3$ nanosheets	GCE	329 (20)	69	1 M KOH	ACS Catal. 2017, 7, 8549
$FeNi_3$@GR@Fe-NiOOH	GCE	280 (5)	65	0.1 M KOH	J. Mater. Chem. A 2016, 4, 7762
Fe doped $NiSe_2$	GCE	227	37.87	1 M KOH	Nanoscale 2017, 9, 6821
NiFeP microflowers	Ni foam	219 (20)	57	1 M KOH	J. Mater. Chem. A 2017, 5, 11229

Fe:Ni/Ni_2P	Ti foil	285 (20)	48	1 M KOH	J. Mater. Chem. A 2017, 5, 14873
Fe-NiSe nanowires	Ni foam	233	48	1 M KOH	J. Mater. Chem. A 2017, 5, 14639
Fe-Ni_3S_2 nanosheets	FeNi alloy foils	282	54	1 M KOH	Small 2017, 13, 1604161
Fe-doped Ni_3C nanodots in N-doped carbon nanosheets	GCE	275	62	1 M KOH	Angew. Chem. Int. Ed. 2017, 56, 12566
Ni_3Fe/N-C sheets	GCE	370	77	0.1 M KOH	Adv. Energy Mater. 2016, 1601172
$Ni_3FeAl_{0.91}$-LDH	Ni foam	304 (20)	57	1 M KOH	Nano Energy 2017, 35, 350
Ni-Fe mixed diselenide cubic nanocages	GCE	240	24	1 M KOH	Adv. Mater. 2017, 29, 1703870
NiFe/$NiCo_2O_4$ nanosheet arrays	Ni foam	105	38.8	1 M KOH	Adv. Funct. Mater. 2016, 26, 3515
layered $Na_{1x}Ni_yFe_{1y}O_2$ double oxide	GCE	290	44	1 M KOH	Energy Environ. Sci. 2017, 10, 121
Cr-doped $Ni_{0.75}Fe_{0.25}(OH)_{2.25}$	GCE	235	39	1 M KOH	J. Phys. Chem. C 2017, 121, 21962
NiFe@NC	GCE	350	56	0.1M KOH	Nano Energy 2016, 30, 426
Pt-NiFe LDH	GCE	230	51	1 M KOH	Nano Energy 2017, 39, 30
NiFe@NC	GCE	258	60	1 M KOH	Nano Energy 2017, 39, 245
S-$NiFe_2O_4$	Ni foam	279	36.7	1.0 M KOH	Nano Energy 2017, 40, 264
Ni_2Fe_1 nanofoams	GCE	190	68	1 M KOH	Nano Energy 2018, 44, 319
mesoporous $Ni_{1-x}Fe_xO_y$ nanorods	GCE	302	42	1 M KOH	Nano Res. 2017, 10, 6, 2096
hypophosphite-intercalated NiFe-LDH	GCE	215 (2)	37.7	1 M KOH	Nano Res. 2017, 10, 5, 1732
sandwichlike NiFe/C	GCE	210 (2)	30	1 M KOH	ACS Appl. Mater. Interfaces 2015, 7, 9203
NiFeP	GCE	277	---	1 M KOH	ACS Appl. Mater. Interfaces 2016, 8, 12798
NiFe-LDH HMS	Ni foam	239	53	1 M KOH	ACS Appl. Mater. Interfaces 2016, 8, 33697
FeNi LDH@NWSSF	NWSSF	210	56	1 M KOH	ACS Appl. Mater. Interfaces 2017, 9, 40281
sandwiched NiFe/C arrays	Ni foam	200 (2)	30	1 M KOH	ACS Catal. 2016, 6, 4477
NiFe@NC_x	GCE	230	60.6	0.1 M KOH	ACS Catal. 2016, 6, 6335
NiFe/NiFe:Pi	CFP	290	38	1 M KOH	ACS Catal. 2017, 7, 2535
$Ni_2P(O)/Fe_2P(O)$	Ni foam	179	42.7	1 M KOH	ACS Energy Lett. 2017, 2, 2257
$Ni(OH)_2$/NiAl	NiAl foil	289	78	1 M KOH	Adv. Sci. 2017, 4, 1700084
CQD/NiFe LDH	GCE	235	30	1 M KOH	ACS Appl. Mater. Interfaces 2014, 6, 7918

NiFeMo nanosheets	Ni foam	280	40	1 M KOH	J. Mater. Chem. A 2015, 3, 16348
NiFe-LDHs	Ni foam	325	44	0.1 M KOH	J. Mater. Chem. A 2015, 3, 16183
NiFe-LDH array	Ni foam	290	31	1 M NaOH	J. Mater. Chem. A 2016, 4, 167
NiFe-LDHs/GSH	GCE	350	54	0.1 M KOH	J. Mater. Chem. A 2015, 3, 24540
NiFe/$NiFeO_x$	GCE	340	34	0.1 M KOH	Chem. Commun. 2016, 52, 11803
Cu@NiFe LDH	Cu foams	310	27.8	1 M KOH	Energy Environ. Sci. 2017, 10, 1820
carbon-supported NiFe layered double hydroxides	GCE	265	56	1 M KOH	Nanoscale 2017, 9, 11596
amorphous NiFe(oxy)hydroxide nanosheet	Graphite foil	214	21	1 M KOH	J. Mater. Chem. A 2017, 5, 24208
NiFeS	GCE	286	56.3	0.1 M KOH	Small 2017, 13, 1700610

Abbreviations: GCE = Glassy carbon electrode; CFP = Carbon fiber paper; CC = Carbon cloth; CP = Carbon paper; NWSSFs: nonwoven stainless steel fabrics; GSH = graphene/single-walled CNT hybrids; NC = N-doped carbon; LDH = Layered double hydroxide; CQD = carbon quantum dot.

Table S3. Comparison of OER performance of F@$FeNi_3$-CC-3 at large current density with recently reported Fe- and Ni-based electrocatalysts in alkaline electrolyte.

Catalysts	Substrate	η at 100 mA·cm^{-2} (mV)	Tafel slope (mV/dec)	Electrolyte	Reference
F@$FeNi_3$-CC-3	***CC***	***270***	***47***	***1.0 M KOH***	***This work***
Ni_3Se_2 nanoforest	Ni foam	353	144	1.0M KOH	Nano Energy 2016, 24,103
NiFe film	Ni foil	300	---	1 M NaOH	ACS Catal. 2016, 6, 1159
amorphous-like Ni-Fe-S ultrathin nanosheets	Ti plate	300	39	1 M KOH	Adv. Sci. 2017, 4, 1600343
Fe-doped Ni_2P nanosheet arrays	Ni foam	214 (50)	55.9	1 M KOH	Adv. Funct. Mater. 2017, 1702513
$Fe_{0.1}NiS_2$ nanoarray	Ti mesh	231	43	1 M KOH	Nano Res. 2016, 9, 11, 3346
EG/$Co_{0.85}Se$/NiFe-LDH	graphite foil	270 (150)	57	1 M KOH	Energy Environ. Sci. 2016, 9, 478
FeOOH/CeO_2 heterolayered nanotube	Ni foam	350 (140)	---	1 M NaOH	Adv. Mater. 2016, 28, 4698
NiS	Ni foam	335 (50)	89	1 M KOH	Chem. Commun. 2016, 52, 1486
Pt-NiFe LDHs	GCE	284 (50)	33	1 M KOH	Nano Energy 2017, 39, 30
Ni_2Fe_1 nanofoams	GCE	270	68	1 M KOH	Nano Energy 2018, 44, 319
NiFe-LDH hollow microsphere	Ni foam	300 (71.7)	53	1M KOH	ACS Appl. Mater. Interfaces 2016, 8, 33697
NiFe-LDH/$NiCo_2O_4$	Ni foam	290 (50)	50	1 M KOH	ACS Appl. Mater. Interfaces 2017, 9, 1488
$NiCo_2S_4$@NiFe LDH	Ni foam	201 (60)	46.3	1 M KOH	ACS Appl. Mater. Interfaces 2017, 9, 15364
NiFe LDH@Au	Ni foam	221 (50)	48.4	1 M KOH	ACS Appl. Mater. Interfaces 2017, 9, 19807
Fe-doped CoP nanoarray	Ti foil	310	67	1M KOH	Adv. Mater. 2017, 28, 1602441
Fe-Pi	Ni foam	257	28	1M KOH	J. Mater. Chem. A 2017, 5, 18627
Fe-Ni phosphide nanoparticle-stack array	Ni foam	186	57	1 M KOH	J. Mater. Chem. A 2017, 5, 13329
$NiFeO_x$	Ni foam	260	28	1 M KOH	ACS Catal. 2016, 6, 6987
NiFe	Ni foam	290	---	1 M KOH	ChemSusChem 2016, 9, 1
NiFe/Cu_2O nanowires	Cu foam	260	42	1M KOH	ChemSusChem 2017, 10, 1475

Abbreviations: GCE = Glassy carbon electrode; LDH = Layered double hydroxide.

Table S4. Parameters obtained by fitting the impedance spectra of F@$FeNi_3$-CC-x and FeOOH-CC using the equivalent circuit in ***Figure 5B***.

Samples	Ws [Ω cm^2]	R_s [Ω cm^2]	R_c [Ω cm^2]
F@$FeNi_3$-CC-1	**1.461**	**122.2**	**1.028**
F@$FeNi_3$-CC-2	**1.021**	**146**	**0.954**
F@$FeNi_3$-CC-3	**0.808**	**96.39**	**0.877**
F@$FeNi_3$-CC-4	**1.167**	**125.4**	**0.905**
FeOOH-CC	**1.561**	**221.2**	**1.205**
F-Fe-CC	**1.451**	**115.1**	**0.7405**